PROCEEDINGS OF SCIENCE

How Cosmic Rays Reshape Their Accelerators

Rebecca Diesing,[a,b,*] **Siddhartha Gupta,**[c] **Minghao Guo,**[c] **Chang-Goo Kim,**[c] **James Stone**[a] **and Damiano Caprioli**[d,e]

[a] *School of Natural Sciences, Institute for Advanced Study, Princeton, NJ 08540, USA*
[b] *Department of Physics and Columbia Astrophysics Laboratory, Columbia University, New York, NY 10027, USA*
[c] *Department of Astrophysical Sciences, Princeton University, Princeton, NJ 08540, USA*
School of Natural Sciences, Institute for Advanced Study, Princeton, NJ 08540, USA
[d] *Department of Astronomy and Astrophysics, The University of Chicago, Chicago, IL 60637, USA*
[e] *Enrico Fermi Institute, The University of Chicago, Chicago, IL 60637, USA*

E-mail: rrdiesing@ias.edu

Cosmic rays (CRs) accelerated at the forward shocks of supernova remnants (SNRs) likely constitute the majority of the Galactic CR population. They also play a vital role in regulating the hydrodynamical evolution of their accelerators. For example, efficient CR acceleration at shocks leads to enhanced compression, which in turn alters the distribution of CRs released into the Galaxy. Galactic CRs can also extend the lives of SNRs, serving as a non-thermal pressure reservoir that supports expansion after the onset of the so-called ”radiative phase," when thermal gas pressure is lost to atomic transitions. In this proceeding, we explore the dynamical role of CRs in regulating SNR evolution, and introduce observational evidence for CRs modifying the hydrodynamics of their accelerators. In particular, by coupling magnetohydrodynamic simulations of SNR evolution with a self-consistent model of CR acceleration at shocks, the presence of both CRs and magnetic fields (which are themselves amplified by CRs) can drastically alter the both the radio and γ-ray appearance of a radiative SNR. Proper accounting for the dynamical effects of both CRs and magnetic fields is essential to producing simulated SNRs that are consistent with multi-wavelength observations.

39th International Cosmic Ray Conference (ICRC2025)
15–24 July 2025
Geneva, Switzerland

ICRC 2025
The Astroparticle Physics Conference
Geneva July 15-24, 2025

*Speaker

PoS(ICRC2025)034

1. Introduction

In the standard picture, supernova remnants (SNRs) are the primary source of cosmic rays (CRs) in our Galaxy [e.g., 6, 20], efficiently accelerating particles via diffusive shock acceleration [DSA, e.g., 3, 5, 8, 16, 23]. This particle acceleration gives rise to nonthermal emission that extends from radio to γ-rays and has been observed extensively [e.g., 1, 25, 29]. Supernova remnants (SNRs) also play a critical role in galaxy formation and evolution by injecting energy and momentum into the interstellar medium (ISM). This injection can drive large-scale winds which quench star formation and enrich the intergalactic medium with metals [e.g., 19]. To model these effects, galaxy formation simulations rely on subgrid prescriptions for SNR "feedback" [see 11] for a recent review].

In order to properly tune these feedback prescriptions, SNR evolution has been studied in a variety of environments [e.g., 21]. While the precise nature of SNR evolution has been shown to depend on the properties of the ambient interstellar medium (ISM), the life of an SNR can be broadly separated into three main phases: I) a free-expansion, or "ejecta-dominated" phase [e.g., 31], which persists until the swept-up mass becomes comparable to the ejecta mass; II) an adiabatic, or "Sedov-Taylor" phase [28, 30], which continues until the shock slows such that the postshock temperature drops below $\sim 10^6$ K and cooling becomes efficient; and III) a "radiative" phase, in which thermal gas loses its energy via atomic transitions and expansion continues first due to the SNR's internal pressure and then due to momentum conservation [e.g., 4, 10, 15].

One of the key predictions of this evolutionary picture is the formation, at the onset of the radiative phase, of a dense shell behind the shock, resulting from the drop in thermal pressure support. [e.g., 7, 26]. This shell formation occurs after roughly $1 - 5 \times 10^4$ yr [for typical ISM densities, e.g., 21] and, in the standard hydrodynamical picture, leads to density enhancement factors approaching $\sim 10^2$ relative to the ambient medium, depending on the shock Mach number [see, e.g., 13, 21, for some useful estimates]. However, a definitive detection of such a shell is still missing. Searches have been conducted using neutral hydrogen emission, but only partial shells have been reported in the literature [see, e.g., 22].

In short, observations point toward a picture in which shell formation is inhibited. As hydrodynamic instabilities appear insufficient to destroy radiative shells on $\sim 10^5$ yr timescales [17], we instead look to nonthermal pressure contributions: CRs and magnetic fields. CRs, which can represent as much as $\sim 10 - 20\%$ of the SNR bulk kinetic energy [9], are known to impact SNR evolution during the radiative stage [12]. Namely, as their energy is not radiated away at late times, they represent a reservoir of pressure available to continue SNR expansion and/or to prevent the formation of the dense shell. By extending the lives of their accelerators, CRs may meaningfully enhance SNR feedback. Similarly, magnetic fields are known to impede shell formation when oriented perpendicular to the shock normal; these perpendicular components are compressed, increasing the magnetic pressure in the vicinity of the shell [27]. However, the combined effect of CR and magnetic pressure–particularly with realistic $\sim 3\mu G$ ambient magnetic fields and a theoretically-motivated picture of CR transport–has not been investigated in the literature.

In this work, we use two-fluid magneto-hydrodynamic (MHD) simulations to model the evolution of an SNR through the radiative phase, including the dynamical effects of both CRs and magnetic fields. We then quantify the impacts of CR acceleration and magnetic compression on shell formation, and couple these simulations with a semi-analytic model of particle acceleration

to predict the nonthermal emission from SNRs with different CR acceleration efficiencies and magnetic field orientations.

2. Method

Herein we describe the model we use to explore the effects of CRs and magnetic fields on a typical SNR as it evolves from adiabatic to radiative. Throughout this work, we consider a representative case with initial energy $E_{\rm SN} = 10^{51}$ erg and ejecta mass $M_{\rm ej} = 1 M_\odot$, expanding into a uniform ISM with number density $n_{\rm ISM} = 1$ cm^{-3}, temperature $T = 10^4$ K, solar metallicity, and perpendicular magnetic field (relative to the shock normal) $B_\perp = B_0 \sin\theta \in [0, 3]\mu$G.

2.1 MHD simulations

To model shock evolution and shell formation, we conduct one-dimensional, spherically symmetric, ideal MHD simulations of a single supernova explosion without thermal conduction or mixing diffusion. As this work concerns radiative SNRs, we neglect the ejecta-dominated stage (and any associated explosion dynamics). More specifically, we use the `PLUTO` code [24], modified to include CRs as an additional fluid component as described in detail in [18].

Note that we neglect CR diffusion and consider only advection, which dominates transport for the ∼GeV particles contributing to the majority of the CR pressure. We also neglect CR cooling due to proton-proton losses, since the loss timescale even in dense environments ($n_{\rm H} \simeq 10^2$ cm^{-3}) far exceeds the SNR ages considered in this work.

2.2 Nonthermal emission

In order to assess the observational consequences of nonthermal pressure during late-stage SNR evolution, we couple our MHD simulations with a detailed calculation of particle acceleration and nonthermal emission described in [13]. Namely, we model CR acceleration using a semi-analytic prescription that self-consistently solves the steady-state transport equation for the distribution of nonthermal particles at the forward shock, including the effects of magnetic field amplification and shock modification due to the presence of CRs.

Our particle acceleration model yields the instantaneous spectrum of protons accelerated at each timestep of our MHD simulations. We convert this spectrum to an instantaneous electron spectrum using the analytical approximation calculated in [33]. To account for energy losses–adiabatic, proton-proton (hadrons only), and synchrotron (electrons only)–we shift and weight our instantaneous spectra as in [13]: each spectrum is treated as a shell of particles that expands according to the velocity profiles given by our MHD simulations. We then apply energy losses (and calculate nonthermal emission) based on the density and magnetic field at each shell's current location. To calculate the spectral energy distribution (SED) of photons produced by our weighted particle distributions, we use the radiative processes code `naima` [32], which computes emission due to synchrotron, bremsstrahlung, inverse Compton (IC) and neutral pion decay processes for each shell of CRs.

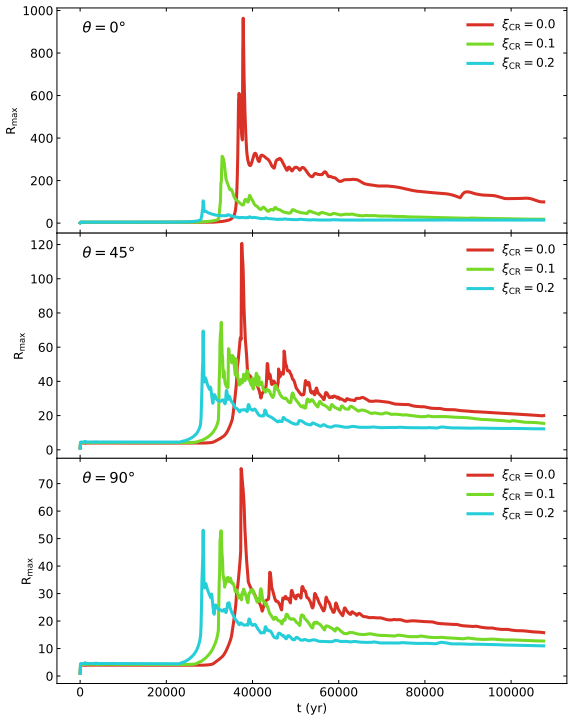

Figure 1: The maximum compression ratio, $R_{\rm max} \equiv \max[\rho(r)/\rho_0]$ as a function of shock age for our representative SNR. Each panel corresponds to a different inclination, θ, of the magnetic field (taken to be 3 μG) with respect to the shock normal, while line color denotes the CR acceleration efficiency, $\xi_{\rm CR}$. Under the right conditions, CRs and magnetic fields can decrease shell densities by up to an order of magnitude.

3. Results

3.1 Shock hydrodynamics

To summarize the effect of CR and magnetic pressures on shell formation, we show the maximum compression ratio, $R_{\rm max} \equiv \max[\rho(r)/\rho_0]$ as a function of shock age in Figure 1. Each panel corresponds to a different magnetic field obliquity θ while color denotes the CR acceleration efficiency, $\xi_{\rm CR}$. We see that increasing $\xi_{\rm CR}$ from 0.0 to 0.2 decreases $R_{\rm max}$ by a factor of ~ 10. Meanwhile, as one increases θ from 0° to 90° (assuming $\xi_{\rm CR} = 0.0$), $R_{\rm max}$ declines by a similar amount. Thus, both CRs and magnetic fields can reduce the shell density. Keep in mind that we consider only the typical ISM value of $B_0 = 3\mu G$; shell densities could be further suppressed in the presence of mild magnetic field amplification or a more highly magnetized medium. We also note that Figure 1 shows that the effect of increasing $\xi_{\rm CR}$ decreases as θ increases. Namely, if one raises $\xi_{\rm CR}$, one lowers $R_{\rm max}$, thereby reducing the maximum magnetic pressure. Similarly, if one raises θ, CRs experience less compression, and therefore provide less pressure support in the vicinity of the shell. In other words, the combined effect of CRs and magnetic fields is highly nonlinear. However, in practice, one would expect efficient CR acceleration only in quasi-parallel (small θ) regions [recall 9]. As such CRs and magnetic fields can provide a reasonably even reduction in shell density across the surface of an SNR, with CRs providing pressure support where θ is small, and magnetic fields providing pressure support where θ is large.

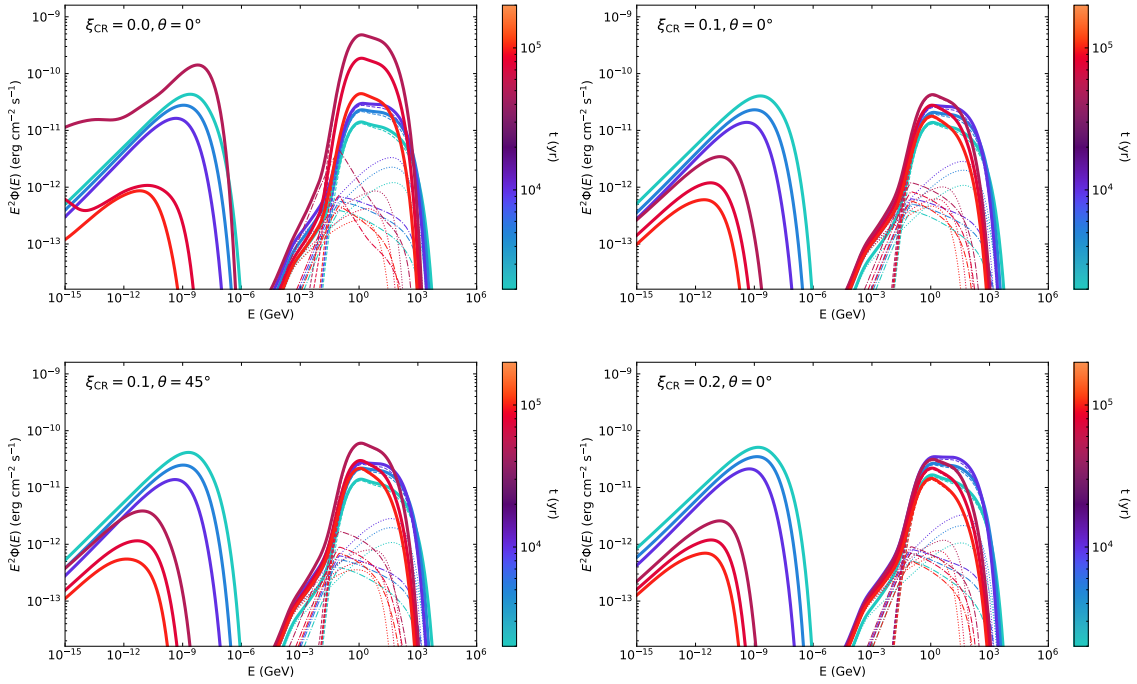

Figure 2: Nonthermal multi-wavelength SEDs from our representative SNR at a distance of 3 kpc. Each panel corresponds to a different magnetic field orientation and/or CR acceleration efficiency. The color scale denotes the age of the SNR, while line styles indicate different emission mechanisms: dashed corresponds to pion decay (hadronic emission), dot-dashed corresponds to nonthermal bremsstrahlung, and dotted corresponds to inverse Compton. Thick lines correspond to total emission, which is dominated by synchrotron at low energies (radio to X-rays) and pion decay at high energies (γ-rays).

3.2 Observational impacts

A sample of nonthermal spectral energy distributions (SEDs) from radio to γ-rays are shown in Figure 2, with each panel corresponding to a different ξ_{CR} and/or θ. The color scale denotes the age of the SNR. Clearly, the case with no dynamical impact from CRs or magnetic fields ($\xi_{CR} = 0.0$ and $\theta = 0°$, top left panel of Figure 2) is unique, exhibiting a dramatic rise in both radio and γ-rays at the onset of the radiative phase. While the synchrotron emission falls off as the shock age approaches 10^5 yr, largely due to strong synchrotron losses in the compressed amplified magnetic field (recall that we use this turbulent field as the target for synchrotron emission), the γ-ray emission remains enhanced out to $t = 10^5$ yr. Notably, this γ-ray emission is so large that TeV emission becomes non-negligible, despite the very conservative estimates of the maximum proton energy considered in this work. Namely, the rise is sufficient to generate appreciable emission above the high-energy cutoff.

On the other hand, the presence of CRs mitigates this enhancement, with no appreciable rise in synchrotron emission and only a modest rise in the nonthermal γ-rays around the onset of the radiative phase; this γ-ray emission quickly decays to emission that resembles Sedov-Taylor levels. This impact can be seen more clearly in Figure 3, which displays nonthermal light curves of our representative SNR in radio (top panel), GeV γ-rays (middle panel), and TeV γ-rays (bottom panel).

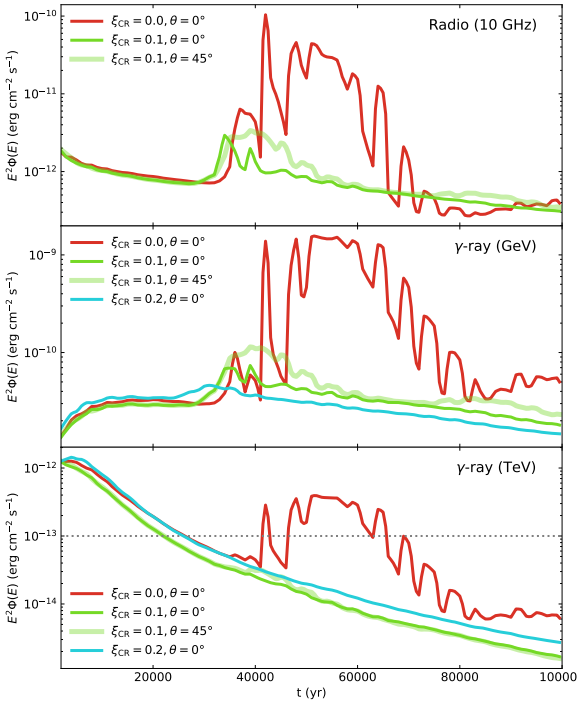

Figure 3: Nonthermal light curves for our representative SNR at a distance of 3 kpc. Each panel represents a different photon energy, while line thickness and color denote the magnetic field orientation and acceleration efficiency, respectively. For comparison purposes, CTA's predicted differential point source sensitivity at 1 TeV is denoted with a gray dotted line on the bottom panel [2]. The presence of CRs reduces not only the magnitude of the nonthermal rebrightening at the onset of the radiative stage, but also its duration.

4. Summary

In short, CRs and magnetic fields can meaningfully alter SNR evolution and emission. In particular, the dearth of radiative SNRs exhibiting bright emission with complete, shell-like morphologies represents circumstantial evidence for inhibited shell formation, likely due to the nonthermal pressure sources described in this work. For additional details, please see [13] and [14].

References

[1] M. Ackermann et al. Detection of the Characteristic Pion-Decay Signature in Supernova Remnants. *Science*, 339:807–811, Feb. 2013.

[2] M. Actis, G. Agnetta, F. Aharonian, A. Akhperjanian, J. Aleksić, E. Aliu, D. Allan, I. Allekotte, F. Antico, L. A. Antonelli, and et al. Design concepts for the Cherenkov Telescope Array CTA: an advanced facility for ground-based high-energy gamma-ray astronomy. *Experimental Astronomy*, 32:193–316, Dec. 2011.

[3] W. I. Axford, E. Leer, and G. Skadron. Acceleration of Cosmic Rays at Shock Fronts (Abstract). In Acceleration of Cosmic Rays at Shock Fronts, volume 2 of *International Cosmic Ray Conference*, pages 273–+, 1977.

[4] R. Bandiera and O. Petruk. A statistical approach to radio emission from shell-type SNRs. I. Basic ideas, techniques, and first results. , 509:A34, Jan. 2010.

[5] A. R. Bell. The acceleration of cosmic rays in shock fronts. I. *MNRAS*, 182:147–156, Jan. 1978.

[6] E. G. Berezhko and H. J. Völk. Spectrum of Cosmic Rays Produced in Supernova Remnants. , 661:L175–L178, June 2007.

[7] G. S. Bisnovatyi-Kogan and S. A. Silich. Shock-wave propagation in the nonuniform interstellar medium. *Reviews of Modern Physics*, 67:661–712, July 1995.

[8] R. D. Blandford and J. P. Ostriker. Particle acceleration by astrophysical shocks. *ApJL*, 221:L29–L32, Apr. 1978.

[9] D. Caprioli and A. Spitkovsky. Simulations of Ion Acceleration at Non-relativistic Shocks: I. Acceleration Efficiency. , 783:91, Mar. 2014.

[10] D. F. Cioffi, C. F. McKee, and E. Bertschinger. Dynamics of radiative supernova remnants. , 334:252–265, Nov. 1988.

[11] R. A. Crain and F. van de Voort. Hydrodynamical simulations of the galaxy population: Enduring successes and outstanding challenges. *Annual Review of Astronomy and Astrophysics*, 61(Volume 61, 2023):473–515, 2023.

[12] R. Diesing and D. Caprioli. Effect of cosmic rays on the evolution and momentum deposition of supernova remnants. *Physical Review Letters*, 121(9):091101, Aug. 2018.

[13] R. Diesing, M. Guo, C.-G. Kim, J. Stone, and D. Caprioli. Nonthermal signatures of radiative supernova remnants. *The Astrophysical Journal*, 974(2):201, oct 2024.

[14] R. Diesing and S. Gupta. Nonthermal Signatures of Radiative Supernova Remnants. II. The Impact of Cosmic Rays and Magnetic Fields. , 980(2):167, Feb. 2025.

[15] B. T. Draine. *Physics of the Interstellar and Intergalactic Medium*. 2011.

[16] E. Fermi. Galactic Magnetic Fields and the Origin of Cosmic Radiation. *Ap. J.*, 119:1–+, Jan. 1954.

[17] M. Guo, C.-G. Kim, and J. M. Stone. Evolution of Supernova Remnants in a Cloudy Multiphase Interstellar Medium. *arXiv e-prints*, page arXiv:2411.12809, Nov. 2024.

[18] S. Gupta, P. Sharma, and A. Mignone. A numerical approach to the non-uniqueness problem of cosmic ray two-fluid equations at shocks. , 502(2):2733–2749, Apr. 2021.

[19] T. M. Heckman and T. A. Thompson. A brief review of galactic winds. *ArXiv e-prints*, Jan. 2017.

[20] A. M. Hillas. TOPICAL REVIEW: Can diffusive shock acceleration in supernova remnants account for high-energy galactic cosmic rays? *Journal of Physics G Nuclear Physics*, 31:95–+, May 2005.

[21] C.-G. Kim and E. C. Ostriker. Momentum injection by supernovae in the interstellar medium. , 802:99, Apr. 2015.

[22] B.-C. Koo, C.-G. Kim, S. Park, and E. C. Ostriker. Radiative Supernova Remnants and Supernova Feedback. , 905(1):35, Dec. 2020.

[23] G. F. Krymskii. A regular mechanism for the acceleration of charged particles on the front of a shock wave. *Akademiia Nauk SSSR Doklady*, 234:1306–1308, June 1977.

[24] A. Mignone, G. Bodo, S. Massaglia, T. Matsakos, O. Tesileanu, C. Zanni, and A. Ferrari. PLUTO: A numerical code for computational astrophysics. , 170(1):228–242, may 2007.

[25] G. Morlino and D. Caprioli. Strong evidence for hadron acceleration in Tycho's supernova remnant. *A&A*, 538:A81, Feb. 2012.

[26] J. P. Ostriker and C. F. McKee. Astrophysical blastwaves. *Reviews of Modern Physics*, 60:1–68, 1988.

[27] O. Petruk, T. Kuzyo, S. Orlando, M. Pohl, M. Miceli, F. Bocchino, V. Beshley, and R. Brose. Post-adiabatic supernova remnants in an interstellar magnetic field: oblique shocks and non-uniform environment. , 479(3):4253–4270, Sept. 2018.

[28] L. I. Sedov. *Similarity and Dimensional Methods in Mechanics*. 1959.

[29] P. Slane, S.-H. Lee, D. C. Ellison, D. J. Patnaude, J. P. Hughes, K. A. Eriksen, D. Castro, and S. Nagataki. A cr-hydro-nei model of the structure and broadband emission from tycho's supernova remnant. , 783:33, Mar. 2014.

[30] G. Taylor. The Formation of a Blast Wave by a Very Intense Explosion. I. Theoretical Discussion. *Proceedings of the Royal Society of London Series A*, 201(1065):159–174, Mar. 1950.

[31] J. K. Truelove and C. F. Mc Kee. Evolution of non-radiative SNRs *[Erratum:* **128** ApJS *(2000) 403]. ApJ Supplement Series*, 120:299–326, Feb. 1999.

[32] V. Zabalza. naima: a python package for inference of relativistic particle energy distributions from observed nonthermal spectra. *Proc. of International Cosmic Ray Conference 2015*, page 922, 2015.

[33] V. N. Zirakashvili and F. Aharonian. Analytical solutions for energy spectra of electrons accelerated by nonrelativistic shock-waves in shell type supernova remnants. *A&A*, 465(3):695–702, 2007.